Nonlinear Normal Modes in
Finite Element Model Validation of
Geometrically Nonlinear Flat and Curved Beams

David A. Ehrhardt[1] and Robert J. Kuether[2]
University of Wisconsin-Madison, Madison, WI, 53706

Matthew S. Allen[3]
University of Wisconsin-Madison, Madison, WI, 53706

Model Validation is an important step in the design of structures operating under dynamic loading. The natural frequencies and mode shapes associated with linear normal modes (LNMs) have been traditionally used to validate and update finite element models, but their usefulness breaks down when a structure operates in a nonlinear response regime. The concept of nonlinear normal modes (NNMs) has been presented as a capable extension of LNMs into nonlinear response regimes. In this work, linear model updating is performed on one flat and one curved beam using the experimentally measured natural frequencies and mode shapes coupled with gradient based optimization. Throughout the updating process, the first NNM of these structures are numerically calculated and compared with the experimentally measured NNM. This comparison is used for model validation throughout each step of the updating procedure. Results show the importance of the definition of initial geometry and effect of the large variation in boundary conditions contributing to changes in the nonlinear behavior of the model.

Nomenclature

$[M]$	=	mass matrix
$[C]$	=	damping matrix
$[K]$	=	stiffness matrix
$\{x(t)\}$	=	displacement vector
$\{\dot{x}(t)\}$	=	velocity vector
$\{\ddot{x}(t)\}$	=	acceleration vector
$f_{nl}(\{x(t)\})$	=	nonlinear force vector
$p(t)$	=	external input force
$\psi_{RB}\, a_b(t)$	=	external inertial loading

I. Introduction

WHEN an engineer is presented with the task to design a structure operating under dynamic loading, a large suite of analysis and test approaches is available. An important step in the design of a structure is connecting results between these analysis and test approaches. This connection, termed model validation, is typically performed in parallel with the alteration of selected parameters of the analysis model to accurately reflect the test results. Current techniques for model validation offer solutions to a wide range of structures operating under complex loading conditions when a structure is in linear response regimes. The term linear is important here since the use of these techniques hinge on the quantification of invariant properties inherent to a structure (e.g., resonant frequencies, damping ratios, mode shapes, etc.). These properties lose their invariance when a structure is in a nonlinear response regime, invalidating the use of established techniques. Therefore, new model validation metrics are sought to

---

[1] Graduate Research Assistant, Engineering Physics, 1415 Engineering Drive, and Student Member.
[2] Graduate Research Assistant, Engineering Physics, 1415 Engineering Drive, and Student Member.
[3] Associate Professor, Engineering Physics, 1415 Engineering Drive, and Lifetime Member.

address structural properties as functions of response amplitude while preserving the simplicity and connection to the linear design and test paradigms.

There is no analysis technique as powerful and widely applicable as the finite element method. Due to the wide range of use, finite element analysis (FEA) techniques capable of solving dynamic problems such as modal analysis, harmonic frequency response, transient dynamic, etc. are readily available. For the calculation of nonlinear normal modes (NNMs), several analytical and numerical techniques are available. Analytical techniques, such as the method of multiple scales [1-4] and the harmonic balance approach [5], are typically restricted to structures where the equations of motion are known in closed form, so analysis is limited to simple geometries. Recently, several new numerical methods have also been developed to calculate NNMs of larger scale structures [6-8] through the use of numerical continuation using MATLAB® coupled with the commercial FEA code Abaqus®. These techniques have recently been extended to calculate the NNMs of geometrically nonlinear finite element models as well [8, 9].

Experimental modal analysis (EMA) techniques have seen extensive development providing a vast amount of possibilities in the measurement of natural frequencies and mode shapes. The most popular and easiest implemented linear experimental modal analysis methods available can be classified as phase separation methods. These methods excite several or all linear normal modes of interest at a single time with the use of broadband or swept-sine excitation, and distinguishes the modes of vibration using the phase relationship between the input force and measured response [10, 11]. These techniques have seen some extension to nonlinear structures [12, 13], and is an active area of research, but these methods were not explored here. A less popular set of EMA techniques are classified as phase resonance testing methods [14-16]. These methods can be more time-consuming than phase separation methods as they focus on single modes of vibration using a multi-point forcing vectors. With phase resonance, a mode of vibration is isolated in a test when the phase relationship between the applied harmonic force and measured displacement response fulfills phase lag quadrature. In other words, all degrees of freedom displace synchronously with a phase lag of 90 degrees from the harmonic input force. These methods have seen successful extension to nonlinear systems [17-19], and are used here to estimate the NNMs of the structure so that model validation can be performed.

Before one can begin validating or updating a model, one must decide which dynamic properties to measure and compare between the FE model and experiment. Linear modal properties are typically used for comparison due their ability to characterize global structural dynamics with a small number of physically meaningful variables. Nonlinear normal modes share these same advantages and so they are used as the basis for model updating in this work. When the comparison between model and experiment reveals that the model is inaccurate, one must determine which parameters or features in the model should be updated to improve the correlation. While brute force approaches based on optimization are used in some applications, in this work we focus on a physics based approach where the only parameters updated are those that are justifiably uncertain. Then, each of those parameters is investigated to see whether they cause important changes in the nonlinear normal modes. Here, nominal dimensions and material properties are used to build an initial model. The calculated and measured natural frequencies are used to update material properties and boundary conditions providing models that better represent the structure's linear dynamics using well established techniques [20]. In the cases shown here, the changes made to the model based on its linear modal parameters may or may not improve the correlation of the nonlinear modes (e.g. the extension of the linear modes to higher energy). Hence, the results show that it is critical to simultaneously consider both the linear and the nonlinear behavior of the model in the model updating process.

The following section reviews the nonlinear normal mode framework that is used in this paper. Then the model updating approach is demonstrated on two structures, a nominally flat and a nominally curved beam with rigid (nominally clamped).

II. Background

A. NNM Numerical Calculation

The concept of nonlinear normal modes (NNMs) has seen much interest due to their usefulness in interpreting a wide class of nonlinear dynamics. The reader is referred to [2, 4, 6, 21] for an in-depth discussion of NNMs in regards to their fundamental properties and methods of calculation.

With the extension of Rosenberg's definition [21] of NNMs to a *not necessarily synchronous periodic motion of the conservative system*, as discussed in [4], NNMs can be calculated using shooting techniques and pseudo arc-length sequential continuation of periodic solutions with step size control as previously discussed in [8]. This method of calculation solves for periodic solutions of the nonlinear equations of motions, presented in Eq. (1), beginning in the linear response range and following the progression of the system response's dependence on input energy. Here, [M] is the mass matrix, [K] is the stiffness matrix, and f_{nl} is the nonlinear restoring force that is a

function of $x(t)$. This method is also capable of following the frequency-energy evolution around sharp changes in the NNM with the ability to track bifurcations, modal interaction, and large energy dependence of the fundamental frequency of vibration. This energy dependence can be presented compactly with the help of a frequency-energy plot (FEP), as seen in Figure 1 for NNM 1 of the two systems of interest for this investigation. In Figure 1, both FEPs are of the baseline model for the nominally flat and curved clamped-clamped beams calculated using the applied modal force method described in [8]. Figure 1a shows the numerically calculated FEP of a nominally flat clamped-clamped beam and demonstrates a spring-hardening effect, or an increase in fundamental frequency of vibration with increasing input energy. Figure 1b shows the FEP of the curved clamped-clamped beam and shows a softening and then a hardening effect. This is characteristic of curved structures where the structure initially approaches the onset of buckling and hence looses stiffness, but then for large deformations the stiffness increases due to coupling between bending and axial stretching [22].

$$[M]\{\ddot{x}(t)\} + [K]\{x(t)\} + f_{nl}(\{x(t)\}) = 0 \tag{1}$$


(a)

(b)
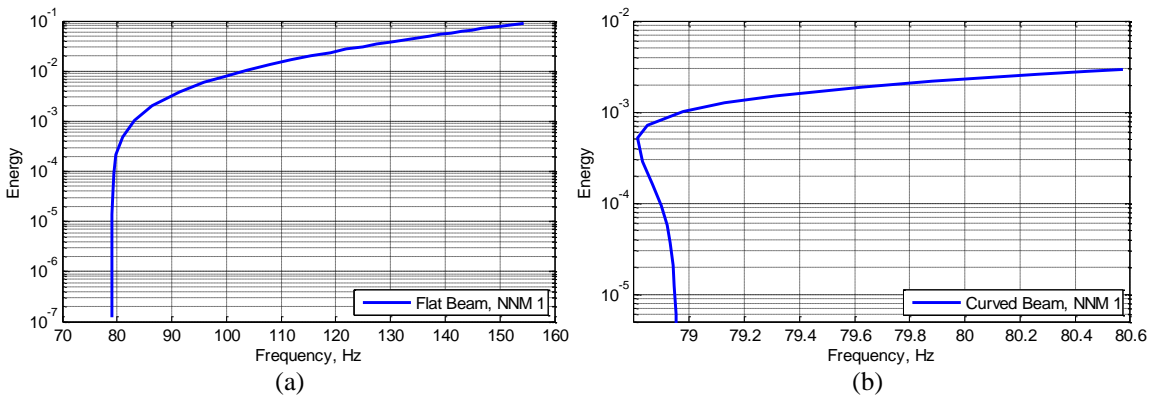
Figure 1: Frequency-Energy Plots Calculated using the Applied Modal Force Method [8]: a) FEP of flat clamped-clamped beam, b) FEP of curved clamped-clamped beam

B. NNM Experimental Measurement

The NNMs of a structure can be measured with the use of force appropriation and an extension of the phase lag quadrature as discussed by Peeters et al. in [17]. They showed that an appropriated multi-point multi-harmonic force can be used to isolate the dynamic response of a structure on an NNM. The nonlinear forced response of a structure with viscous damping can be represented in matrix form by Eq. (2), where [C] is the damping matrix and $p(t)$ is the external excitation. As discussed before, an un-damped NNM is defined as a periodic solution to Eq. (1). So, if the forced response of a structure is on an NNM, then the defined conservative equation of motion is equal to zero, so all that remains is Eq. (3). Therefore, the forced response of a nonlinear system is on an NNM if the input force is equal to the structural damping for all response harmonics. As with linear force appropriation, the appropriated force can be simplified to single-point mono-harmonic components, giving the response in the neighborhood of an NNM, providing a practical application to experimental measurement. This simplification breaks down when the input force is not able to properly excite all modes in the response requiring careful consideration of input force location. This approach was used on the both beams studied in this work as presented in Figure 2. Here, instead of energy, the maximum amplitude of the response is presented as a function of the fundamental frequency of the response. Although the presentation of energy would provide a more complete comparison between analysis and test, examining the maximum amplitude of deformation preserves the expected trends of the nonlinearities without an approximation of the systems energy.

$$[M]\{\ddot{x}(t)\}+[C]\{\dot{x}(t)\}+[K]\{x(t)\}+ f_{nl}(\{x(t)\})= p(t) \tag{2}$$

$$[C]\{\dot{x}(t)\}= p(t) = -[M]\psi_{RB}a_b(t) \tag{3}$$
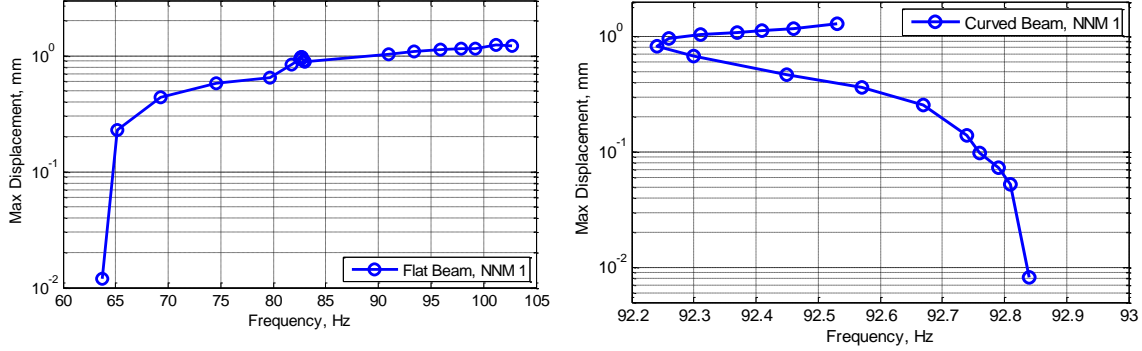
Figure 2: Frequency vs. Max Amplitude Plots: a) Flat clamped-clamped beam,
b) Curved clamped-clamped beam

C. Modeling Considerations

Although beams are considered relatively simple structures, validating the finite element model with experimental measurements involves some engineering judgment and physical insight to the inherent uncertainty of the total physical assembly. For the clamped-clamped beams under investigation, uncertainties in initial geometry, material properties, and boundary conditions are expected to dominate variations in the dynamic response. Therefore, a general model, shown schematically in Figure 3 for the flat beam, is considered. In Figure 3, K_A represents the axial stiffness of the boundary, K_T the transverse stiffness, K_θ the rotational stiffness of the boundary, the black line represents nominal geometry, and the orange line represents the measured initial geometry. The starting point for the model updating procedure uses the nominal geometry (shown in black), nominal material properties, and fixed boundary conditions ($K_A = K_T = K_\theta = $ infinity). Variations in the initial geometry (shown in orange) are taken into account with the use of full-field coordinate measurements of the beam surface. The remaining variation between the model and measurements are accounted for the modulus of elasticity and boundary conditions.
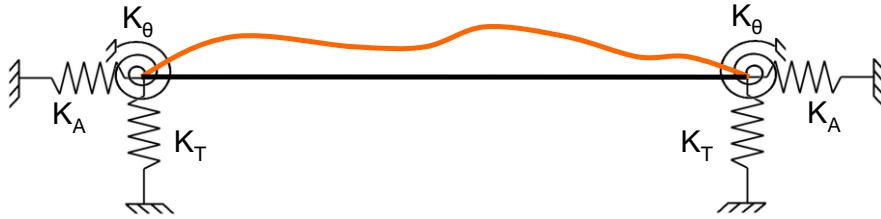

Figure 3: Boundary Condition Schematic

III. Nominally Flat Beam

A. Flat Beam Structure Description

The first structure under test for this investigation is a precision-machined feeler gauge made from high-carbon, spring-steel in a clamped-clamped configuration, as was previously studied in [23]. The beam has an

effective length of 228.6mm, a nominal width of 12.7mm, and a thickness of 0.762mm. All presented dimensions are nominal and subject to variation from clamping and from the machining process to obtain the desired thickness. Prior to clamping, the beam was prepared for three dimensional digital image correlation (3D-DIC) and continuous-scan laser Doppler vibrometry (CSLDV) as discussed in [24] and shown in Figure 4. Locations of the initial laser Doppler vibrometry (LDV) measurements are also shown at the center of the beam and 12mm to the left of the center measurement. The clamping force was provided by the two 6.35-28 UNF-2B bolts located on the inside of the clamping fixture. Before and after clamping the beam in the fixture, static 3D-DIC was used to measure the initial curvature of the clamped beam and the result is shown in Figure 4b. It is interesting to note that although the beam is assumed to be nominally flat, before and after clamping the beam has an initial deflection of 4% and 0.01% of the beam thickness, which is not obvious to the observer. This change of initial curvature has little effect on the linear analyses, but could change the characteristic nonlinearity of the beam (e.g. softening to hardening effect). A 7th order polynomial, shown in Figure 4c, was then fit to the measured curvature and used to approximate the initial geometry. Additionally, single-input single-output modal hammer tests were performed throughout testing on the beam to identify natural frequencies and damping ratios. Results from these hammer tests showed a 5% variation in the first natural frequency of the final clamped beam, which can be expected for this test setup. An average value of the identified natural frequencies, as seen in Table 1, was used for linear model updating.

(a)

(b)

(c)
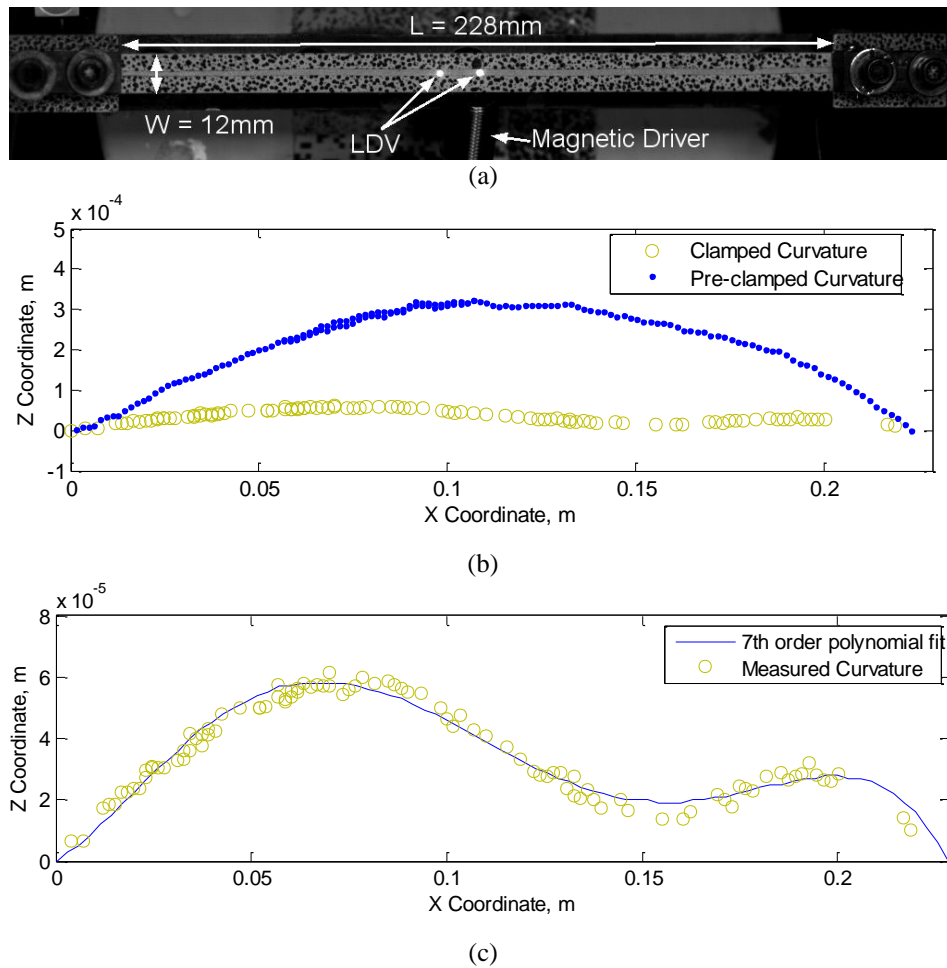
Figure 4: Flat Beam in Clamp: a) XY Plane image of beam, b) measured XZ geometry of beam

B. Flat Beam Linear Comparison

Four finite element models were created to explore the effect of the model parameters on the linear and nonlinear dynamics. All models used 81 Abaqus® beam elements evenly spaced along the x-coordinate of the beam. For each model, linear natural frequencies and mode shapes were calculated and used for comparison with the experimentally measured natural frequencies. The first model created was based on the nominal dimensions previously described and under the assumption of fixed boundary conditions. As seen in Table 1, the natural frequencies of the nominal beam model did not match well with the measured values resulting in large error between the two sets of natural frequencies. The second model created updated the initial geometry of the beam to include the measured curvature of the beam, but the fixed boundary conditions were retained (e.g. $K_A = K_T = K_\theta = $ infinity). The addition of curvature to this model showed a decrease in frequency in all modes and a reduction in percent error when compared with the measured values, but percent errors were still not within ±5%. The third model created took into account variations in boundary conditions by including the axial (K_A), transverse (K_T), and torsion (K_θ) springs at the boundaries schematically shown in Figure 3. Initial values for these springs were based on results from [23] and are shown in Table 2. Adding these springs further lowered the natural frequencies of the FEM of the beam, but percent errors were still out of acceptable ranges, so variation in the elastic modulus and boundary condition springs was allowed to better match the model to the experiment. Using gradient based optimization and constraining the change in modulus to the maximum value in literature, this lead to a factor of 100 increase in the axial and transverse spring values and a factor of 0.5 decrease in the torsion springs value. This updated model brought the error in the natural frequencies within an acceptable range of error for the first four modes as seen in Table 1. Finally, the modulus was allowed to vary from 2.31 GPa to 2.74 GPa, and gradient based optimization was again performed resulting in a factor of 1000 increase in the axial spring, a factor of 0.000001 decrease in the transverse spring, and factor of 0.71 decrease in the torsion spring value. This resulted in smaller frequency error with all but the 5th mode. With the fully updated models, it is interesting to note that the large variation in boundary conditions are not surprising for the clamped-clamped configuration used and can make updating difficult. Also, with the increase of modulus, it is expected that prestress from clamping needs to be accounted.

Mode	Experiment	Nominal Flat Beam	% Error	IC-FF Initial Curvature, fixed-fixed	% Error	IC-NS Initial Curvature, Nominal Boundaries	% Error	IC-US Initial Curvature, Updated Springs	% Error	IC-USM Initial Curvature, Updated Springs/ Modulus	% Error
1	65.05	79.02	21.47	78.18	20.18	76.97	18.32	65.82	1.19	65.31	0.40
2	194.86	217.92	11.84	215.61	10.65	212.29	8.95	189.37	-2.82	193.16	-0.87
3	394.31	427.46	8.41	422.38	7.12	415.98	5.50	382.78	-2.92	394.00	-0.08
4	661.42	707.15	6.91	698.12	5.55	687.67	3.97	647.55	-2.10	665.11	0.56
5	856.16	1057.30	23.49	1042.90	21.81	1027.50	20.01	984.82	15.03	1000.70	16.88
6	995.53	1478.40	48.50	1456.80	46.33	1435.50	44.20	1395.20	40.15	1392.00	39.83
7	1397.83	1970.70	40.98	1939.80	38.77	1911.70	36.76	1879.00	34.42	1827.60	30.75

Table 1: Flat Beam Correlation Results

	E, GPa	K_A, N/m	K_T, N/m	K_θ, N*m/rad
IC-NS	2.00	3.50E+08	5.20E+08	1.13E+02
IC-US	2.31	3.50E+10	3.97E+10	5.65E+00
IC-USM	2.74	1.09E+13	1.71E+05	4.03E+00

Table 2: Updated Elastic Modulus and Spring Values for the Flat Beam

C. Flat Beam Nonlinear Comparison

As the beam's response increases into a nonlinear regime, the fundamental frequency of vibration becomes a function of input energy. Instead of calculating the energy of the beam at increased force levels from the experiment, the directly measured maximum displacement at the center point of the beam is used to create a representative FEP for comparison between analysis and test. The first NNM was calculated for each model created during the model updating process using the applied modal force method [8] and are presented inFigure **5**.Figure 5a shows the representative FEP for each step of the model updating, and emphasizes that as the linear frequency converges to the desired value, the nonlinearity experiences a drastic change in the frequency-energy relationship. By scaling the frequency of the representative FEP to the model's linear natural frequency, this relationship is further emphasized as seen inFigure 5b. Starting with the flat fixed-fixed beam, shown in blue, the nonlinear frequency-energy relation changes with each successive change in the model parameters. The greatest change in the nonlinearity is observed when the initial curvature is added to the model, shown in green. When compared with the flat fixed-fixed beam, the updated geometry changed the first linear natural frequency 1.1% while the frequency-displacement relationship for NNM 1 was reduced by approximately 50% for the input range investigated, showing the sensitivity of the nonlinearity to initial geometry. With the addition of boundary condition springs, the linear model showed a decrease of 1.5% of the first natural frequency, where NNM 1 showed an increase in the frequency-displacement relationship of 5%. This shows that the relationship between the change in linear natural frequency and the nonlinear frequency-displacement relationship is not linear in nature, as expected. The remaining two models showed a larger change in the first linear natural frequency than in the nonlinear portion of the representative FEP. Based on the results of the comparison inFigure 5 and Table 1 it appears that either of the models denoted IC-US or IC-SM should accurately describe the dynamics of the beam when dominated by the first mode. Improved accuracy in the nonlinear region of the model could be made with the inclusion of prestress. Similar comparisons can also be made with higher NNMs if the response is dominated by higher modes.
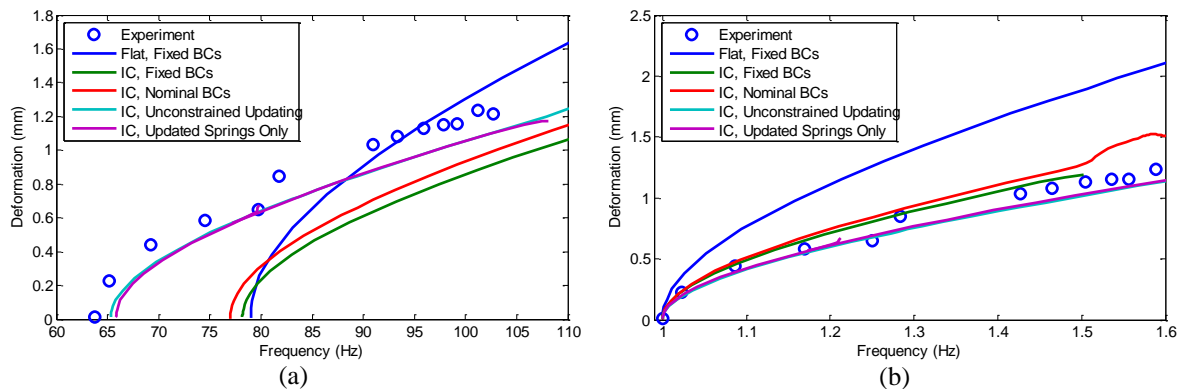

Figure 5: Maximum Displacement Backbone Curves of Center Point of Beam: a) Linear and nonlinear comparison, b) Nonlinear comparison

IV. Nominally Curved Beam

A. Curved Beam Structure Description

The second structure under test for this investigation is a cold rolled curved beam made from high-carbon, spring-steel in a clamped-clamped configuration. The beam has an effective length of 304.85mm, a nominal width of 12.7mm, and a thickness of 0.508mm. The cold rolling was done to induce an initial curvature of 3048mm, but as with the flat beam, all presented dimensions are nominal and subject to variation. The clamping force was provided by the two 6.35-28 UNF-2B bolts located on the inside of the clamping fixture, which is the same fixture used in [25]. Before and after clamping the beam in the fixture, static 3D-DIC was again used to measure the initial curvature of the clamped beam as shown in Figure 6b. It is observed here that the clamping induces an asymmetric preload to the final configuration of the beam, which is not accounted for in the model. Similar to the flat beam, an 8th order polynomial was then fit to the measured curvature and used to approximate the initial geometry of the beam

as shown in Figure 6c. As with the flat beam, single-input single-output modal hammer tests were performed throughout testing on the curved beam to identify natural frequencies and damping ratios. Results from these hammer tests showed a 7% variation in the first natural frequency of the final clamped beam, which can be expected. An average value of the identified natural frequencies, as seen in Table 3, was used for linear model updating.

(a)

(b)

(c)
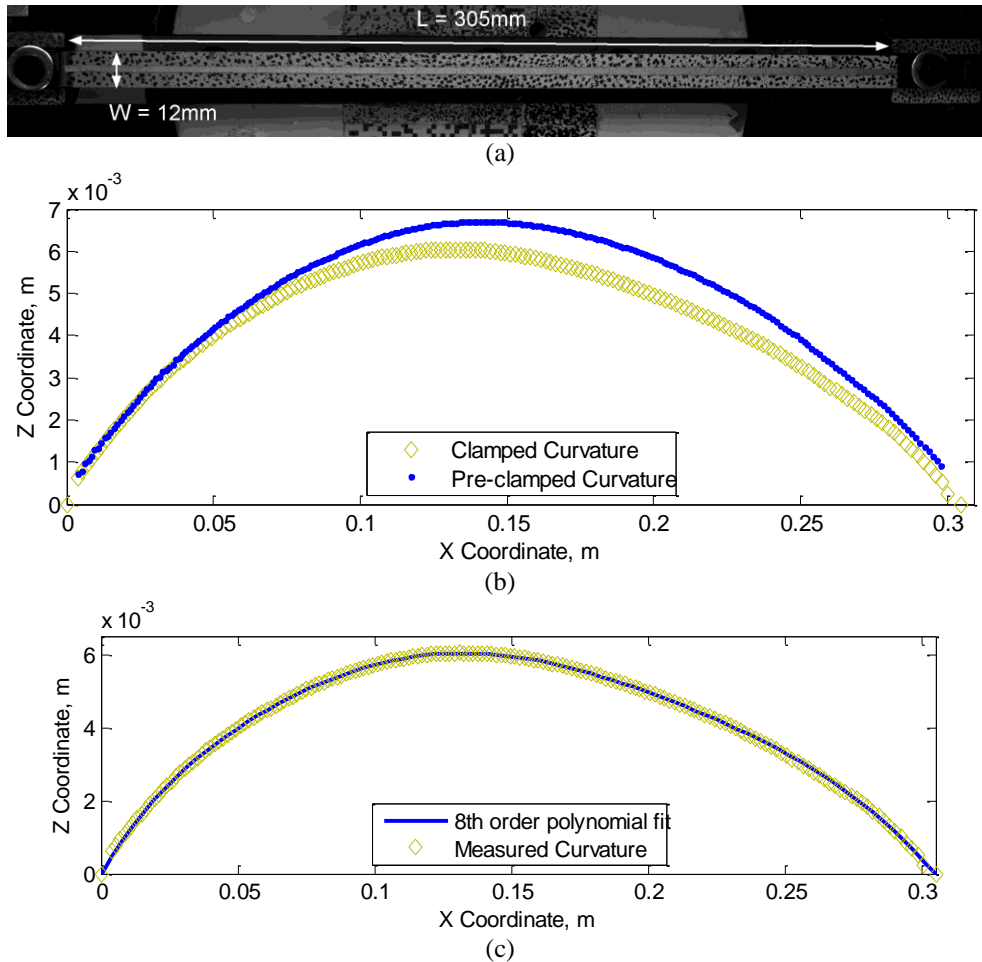
Figure 6: Curved Beam in Clamp: XY Plane image of beam, b) XZ geometry of beam

B.   Curved Beam Linear Comparison

The model updating procedure described for the nominally flat beam was repeated for the nominally curved beam. Again, four finite element models were created and each model used 81 Abaqus® beam elements evenly spaced along the x-coordinate of the beam. For each model, the linear natural frequencies and mode shapes were calculated and used for comparison with the experimentally measured natural frequencies. The first model created was based on the nominal dimensions previously described for the curved beam and under the assumption of fixed boundary conditions. As seen in Table 3, the natural frequencies of the nominal beam model again did not match well with the measured values. The second model created updated the initial geometry of the beam to include the measured curvature of the beam, but the fixed boundary conditions were retained (e.g. $K_A = K_T = K_\theta$ = infinity). The addition of curvature to this model showed an increase in frequency in all modes and a reduction in frequency errors when compared with the measured values, with modes 4 and 5 outside the desired ±5%. Since a similar clamp was used, the third model created used the same nominal values for the boundary condition springs that were used for the

American Institute of Aeronautics and Astronautics

flat beam as shown in Table 4. The addition of these springs had varying effects to the natural frequencies of the beam, but the frequency errors for modes 4 and 5 were still larger than desired, so the elastic modulus and boundary condition springs were varied using gradient based optimization while also constraining the change in modulus to the maximum value in literature. This lead to a factor of 10^7 increase in the axial spring stiffness, a factor of 100 increase in transverse spring, and a factor of 6000 increase in the torsion springs value. This updated model reduced the error in modes 4 and 5, but overall the errors in the natural frequencies are larger than for the model with nominal boundary springs and the large error in the first natural frequency is certainly a concern. Finally, the modulus was allowed to vary from 2.31 GPa to 2.76 GPa, and gradient based optimization was again performed resulting in a factor of 10^5 increase in the axial spring and no change in the transverse and torsion spring values. This updated model brought all natural frequencies within about 2% of the measured values, with many of the frequency errors well below 1%, so no further tuning was attempted.

Mode	Experiment	Nominal Curved Beam	% Error	IC-FF Initial Curvature, fixed-fixed	% Error	IC-NB Initial Curvature, Nominal Boundaries	% Error	IC-US Initial Curvature, Updated Springs	% Error	IC-USM Initial Curvature, Updated Springs/ Modulus	% Error
1	87.33	78.96	-9.59	85.43	-2.18	85.04	-2.62	78.41	-10.22	85.48	-2.12
2	151.48	132.14	-12.77	151.22	-0.17	150.26	-0.81	138.80	-8.37	149.60	-1.24
3	296.03	216.12	-26.99	294.98	-0.36	293.68	-0.79	270.77	-8.53	295.56	-0.16
4	319.72	256.00	-19.93	346.63	8.42	343.67	7.49	318.22	-0.47	318.36	-0.43
5	508.20	387.34	-23.78	559.21	10.04	555.17	9.24	513.34	1.01	511.38	0.63
6	620.41	534.43	-13.86	623.46	0.49	620.77	0.06	572.40	-7.74	620.23	-0.03
7	841.58	712.89	-15.29	873.25	3.76	869.19	3.28	801.77	-4.73	851.01	1.12
8	1057.02	914.52	-13.48	1056.80	-0.02	1052.40	-0.44	970.60	-8.18	1057.80	0.07
9	1326.11	1143.20	-13.79	1340.10	1.05	1334.50	0.63	1231.00	-7.17	1333.50	0.56
10	1583.64	1396.70	-11.80	1609.80	1.65	1603.00	1.22	1479.00	-6.61	1612.90	1.85

Table 3: Curved Beam Correlation Results

	E, GPa	K_A, N/m	K_T, N/m	K_θ, N*m/rad
IC-NB	2.00E+11	3.50E+08	5.20E+08	1.13E+02
IC-US	2.31E+11	1.56E+15	5.20E+10	6.93E+05
IC-USM	2.76E+11	1.79E+11	5.20E+10	6.93E+05

Table 4: Updated Elastic Modulus and Spring Values for the Curved Beam

C. Curved Beam Nonlinear Comparison

As previously shown, the increased curvature in the curved beam induces a change in the nonlinear behavior. The results presented previously in Figure 1, showed that the numerical model and experimental measurement displayed a spring softening to spring hardening characteristic for NNM 1. The comparison between analysis and measurement is shown in Figure 7. Figure 7a shows the un-scaled results emphasizing the discrepancy between the liner and nonlinear part of the NNM. Figure 7b shows the scaled results emphasizing the differences in the nonlinear behavior. As shown in Figure 7b, the nominally curved model, shown with a blue line, and the experiment, shown with blue circles, show a large difference in the "turning point", or change from spring softening to spring hardening, of the characteristic FEP. When the initial curvature of the beam is changed to match the measured shape of the beam, the result shown with a green line reveals that the characteristic of the nonlinearity changes to initially spring hardening and then spring softening; this is the opposite of what is observed experimentally. So, even though this change to the model improves the correspondence of the linear natural frequencies, this comparison reveals that the model now represents the nonlinear behavior less accurately.

The models IC-NB and IC-US with nominal and updated values for the boundary condition springs also predict initial hardening and then softening, further underscoring the fact that updating the model based on its linear behavior alone is not sufficient to bring the nonlinear behavior into agreement. It is also interesting to note that while the large changes (10^7 change in axial spring, 10^2 change in transverse spring, and the 10^3 change in torsion spring) change the location of the turning point in the FEP, the hardening to softening characteristic is maintained; apparently this characteristic is a function of the geometry alone or of some other parameter that was not considered. Finally, consider the model IC-USM where the modulus of elasticity. Although the linear portion of the fully updated model matches experiment well, it does not do any better at capturing the nonlinearity. So, further updating will be needed to bring this model into correspondence with measurements. Considering Figure 6, it could be posed that prestress in the beam due to clamping into the fixture may be important, so it will be allowed to vary in future models.
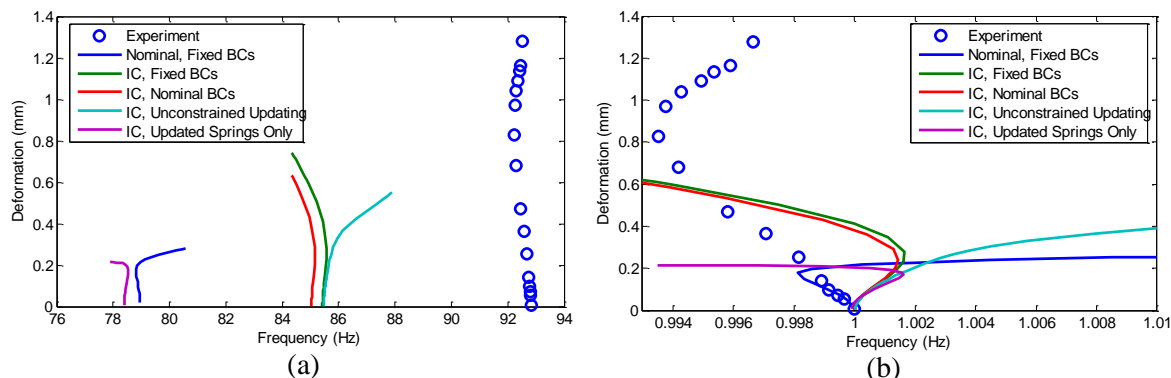
Figure 7: Maximum Displacement Backbone Curves of Quarter Point of Curved Beam: a) Linear and nonlinear comparison, b) Nonlinear comparison

V.   Conclusions

This work has explored the use of NNM backbones as a metric for finite element model validation in nonlinear response regimes for two beam structures. Through the examination of single point responses on each of the beam's surface, the frequency-energy relationship is presented. For the nominally flat beam, the inclusion of this curvature is an important step to the accurate estimation of the nonlinear energy dependence of the fundamental frequency of vibration. Additionally, through the change of boundary conditions, this energy dependence can be tuned to match experimental measurements. Here, it is important to include axial and transverse springs due to the small initial curvature. If the beam was flat, only axial springs would be needed for model updating and tuning of the nonlinearity, but for the presented results, the transverse springs were as significant as the axial springs. For the nominally curved beam, changing the curvature and boundary conditions has been shown to change the fundamental characteristic of the nonlinearity inherent to the structure. Therefore, more care must be taken in the model updating procedure to ensure that the true nonlinearity is accounted.

Future work will seek to add effects from asymmetries and prestress induced from clamping. With the use of NNM force appropriation and full-field measurements, as described in [26], an examination of the effect of asymmetries to the dynamic response is possible. With the examination of the change in mode shapes at higher response levels, more insight can be gained for the improved correlation of the nonlinearity, which would be especially information for structures with complex changes in nonlinearity (e.g. the curved beam). Also, work will seek to use NNM backbones as a quantitative metric for nonlinear model updating using a global metric instead of examining single point responses.

References

[1]   A. H. Nayfeh, *Introduction to Perturbation Techniques*. New York: Wiley, 1981.

[2]   A. F. Vakakis, Manevitch, L.I., Mikhlin, Y.V., Pilipchuk, V.M., and Zeven, A.A., *Normal Modes and Localization in Nonlinear Systems*. New York: John Wiley & Sons, 1996.

[3]   W. Lacarbonara, Rega, G., Nayfeh, A.H., "Resonant Nonlinear Normal Modes Part I: Analytical Treatment for Structural One-dimensional Systems," *International Journal for Nonlinear Mechanics,* vol. 38, pp. 851-872, 2003.

[4]   G. Kerschen, M. Peeters, J. C. Golinval, and A. F. Vakakis, "Nonlinear normal modes, Part I: A useful framework for the structural dynamicist," *Mechanical Systems and Signal Processing,* vol. 23, pp. 170-194, 2009.

[5]   A. H. Nayfeh, *Nonlinear Oscillations*. New York: John Wiley and Sons, 1979.

[6]   M. Peeters, Viguie, R., Serandour, G., Kerschen, G., and Golinval, J.C., "Nonlinear Normal Modes, Part II: Toward a Practical Computation using Numerical Continuation Techniques," *Mechanical Systems and Signal Processing,* vol. 23, pp. 195-216, 2009.

[7]   R. J. Kuether, and Allen, M.S., "Computing Nonlinear Normal Modes using Numerical Continuation and Force Appropriation," in *ASME 2012 International Design Engineering Technical Conferences & Computers and Information in Engineering Conference*, Chicago IL, 2012.

[8]   R. J. Kuether, and Allen, M.S., "A numerical approach to directly compute nonlinear normal modes of geometrically nonlinear finite element models," *Mechanical Systems and Signal Processing,* vol. 46, pp. 1-15, 2014.

[9]   R. J. Kuether, and Allen, M.S., "Nonlinear Modal Substructuring of Systems with Geometric Nonlinearities," in *54th AIAA/ASME/ASCE/AHS/ASC Structures, Structural Dynamics, and Materials Conference*, ed: American Institute of Aeronautics and Astronautics, 2013.

[10]   R. J. Allemang, and Brown, D.L., "A Unifid Matrix Polynomial Approach to Modal Identification," *Journal of Sound and Vibration,* vol. 211, pp. 301-322, 1998.

[11]   D. J. Ewins, *Modal Analysis Theory, Practice, and Application*, Second Edition ed.: Research Studies Press Ltd., 2000.

[12]   K. Worden, and Tomlinson, G.R., *Nonlinearity in Structural Dynamics: Detection, Identification, and Modeling*. Bristol and Philadelphia: Institute of Physics Publishing, 2001.

[13]   G. Kerschen, K. Worden, A. F. Vakakis, and J.-C. Golinval, "Past, present and future of nonlinear system identification in structural dynamics," *Mechanical Systems and Signal Processing,* vol. 20, pp. 505-592, 2006.

[14]   R. C. Lewis, and Wrisley, D.L., "A System for the Excitation of Pure Natural Modes of Complex Structure," *Journal of the Aeronautical Sciences (Institute of the Aeronautical Sciences),* vol. 17, pp. 705-722, 1950/11/01 1950.

[15]   B. Fraeijs de Veubeke, *A variational approach to pure mode excitation based on characteristic phase lag theory*. Paris, France: North Atlantic Treaty Organization, Advisory Group for Aerospace Research and Development, 1956.

[16]   J. R. Wright, J. E. Cooper, and M. J. Desforges, "Normal Mode Force Appropriation - Theory and Application," *Mechanical Systems and Signal Processing,* vol. 13, pp. 217-240, 1999.

[17]   M. Peeters, G. Kerschen, and J. C. Golinval, "Dynamic testing of nonlinear vibrating structures using nonlinear normal modes," *Journal of Sound and Vibration,* vol. 330, pp. 486-509, 2011.

[18]   P. A. Atkins, J. R. Wright, and K. Worden, "AN EXTENSION OF FORCE APPROPRIATION TO THE IDENTIFICATION OF NON-LINEAR MULTI-DEGREE OF FREEDOM SYSTEMS," *Journal of Sound and Vibration,* vol. 237, pp. 23-43, 2000.

[19]   D. A. Ehrhardt, Harris, R.B., and Allen, M.S., "Numerical and Experimental Determination of Nonlinear Normal Modes of a Circular Perforated Plate," in *International Modal Analysis Conference XXXII*, Orlando, Fl, 2014, pp. 239-251.

[20]   M. I. Friswell, and Mottershead, J.E., *Finite Element Model Updating in Structural Dynamics*: Kluwer Academic Publishers, 1995.

[21]   R. M. Rosenberg, "Normal Modes of Nonlinear Dual-Mode Systems," *Journal of Applied Mechanics,* vol. 27, pp. 263-268, 1960.

[22]   L. N. Virgin, *Introduction to Experimental Nonlinear Dynamics: A Case Study in Mechanial Vibration*. Cambridge, United Kingdom: Cambridge University Press, 2000.

[23]   R. W. Gordon, Hollkamp, J.J., and Spottswood, S. M., "Non-linear Response of a Clamped-Clamped Beam to Random Base Excitation," presented at the VIII International Conference on Recent Advances in Structural Dynamics, Southampton, United Kingdom, 2003.

[24]   D. Ehrhardt, S. Yang, T. Beberniss, and M. Allen, "Mode Shape Comparison Using Continuous-Scan Laser Doppler Vibrometry and High Speed 3D Digital Image Correlation," in *International Modal Analysis Conference XXXII*, Orlando, FL, 2014, pp. 321-331.

[25]   J. Abanto-Bueno, Ehrhardt, D., Shukla, A., and Parks, C., "Non-Contact Experimental Modal Analysis of a Curved Beam using a Full-Field Optical Technique," in *52nd AIAA/ASME/ASCE/AHS/ASC Structures, Structural Dynamics and Materials Conference*, ed: American Institute of Aeronautics and Astronautics, 2011.

[26]   D. A. Ehrhardt, Allen, M.S., Beberniss, T.J., "Measurement of Nonlinear Normal Modes using Mono-harmonic Force Appropriation: Experimental Investigation," in *International Modal Analysis Conference 33*, Orlando, FL, 2015.